Trigger Waves in the Acidic Bromate Oxidation of Ferroin

Kenneth Showalter

Department of Chemistry, West Virginia University, Morgantown, West Virginia 26506 (Received: July 21, 1980)

The acidic bromate oxidation of ferroin in batch reaction proceeds with slow consumption of bromide until a critical bromide concentration is attained. At that point ferroin is suddenly oxidized to ferriin in a process involving autocatalytic generation of bromous acid. Prior to the transition, in an unstirred thin film of solution, a single trigger wave of chemical reactivity may develop and subsequently propagate, converting the reaction mixture from the reduced state to the oxidized state. Because the reaction is nonoscillatory, the trigger wave represents a propagating front. Waves were electrochemically initiated by local depletion of bromide and effects of reactant concentrations on propagation velocity were investigated. The dependence of wave velocity on [Br^-] ahead of the advancing wave was investigated and the critical bromide concentration for wave propagation, $[Br^-]_{tw}$, was determined. The coexistence of kinetic states and spatial bistability are considered.

Introduction

Experimental study of chemical wave behavior has been confined primarily to the Belousov[1]–Zhabotinsky[2] (BZ) reaction. Trigger waves[3] represent a particularly fascinating behavior of the BZ reaction. In an unstirred reaction mixture, waves of chemical reactivity travel at an almost constant velocity by triggering their own propagation. Velocity dependence on reactant concentrations has been systematically investigated and explained[4] in terms of the Field–Körös–Noyes (FKN) mechanism[5] for the BZ reaction. Reusser and Field[6] have modeled the reaction-diffusion behavior using the Oregonator,[7] a mathematical model containing the essential kinetic features of the FKN mechanism. A recent study of electrochemical initiation of trigger waves[8] demonstrated that initiation dependence on reactant concentrations and a variety of other features are also accounted for by the FKN mechanism.

A reaction closely related to the oscillating BZ reaction is the acidic bromate oxidation of Ce(III) and other weak one-electron reducing agents. In a batch reactor, the reaction has the features of a clock reaction: a long induction period followed by a sudden oxidation of the metal ion. In a continuously stirred tank reactor (CSTR), the reaction exhibits bistability,[9] and the concentrations of certain intermediate species differ by orders of magnitude in each of the stationary states. The bistability behavior has been modeled[10] almost quantitatively by using bromate chemistry from the FKN mechanism. Noyes[11] has recently developed a reduced model similar to the Oregonator that faithfully reproduces the essential features of the CSTR experiment.

In this paper, we consider the reaction-diffusion behavior of the acidic bromate oxidation of ferroin. Just as trigger wave behavior is the spatial analogue of temporal oscillations in the BZ reaction, trigger wave behavior in the ferroin–bromate system is the spatial analogue of bistability in the CSTR experiment. Because the CSTR bistability occurs in an open system and the reaction-diffusion experiment is by necessity closed, the analogy is imperfect. However, it leads to interesting implications concerning multiple kinetic states in common batch reactions.

We report here a systematic investigation of trigger wave[12] initiation and propagation in the ferroin–bromate system. Local depletion of Br^- in a thin film of solution containing H_2SO_4, $NaBrO_3$, KBr, tris(1,10-phenanthroline)iron(II) sulfate, and 4-cyclohexene-1,2-dicarboxylic acid generates a region of oxidized solution which advances into the surrounding reduced solution, ultimately converting the reaction mixture from the reduced to the oxidized state. Figure 1 shows a trigger wave at 31.5 min that was initiated at ca. 11.5 min after mixing reactants. The blue oxidized region in the center is advancing outward into the orange reduced region.

The Chemical Reaction

The oxidation of weak one-electron reducing agents such as ferroin by acidic bromate is well understood. The reaction sequence (A1)–(B3), extracted from the FKN mechanism,[5] contains the essential kinetic features of the reaction.[10,13,14]

$$BrO_3^- + Br^- + 2\,H^+ = HBrO_2 + HOBr \quad (A1)$$

$$HBrO_2 + Br^- + H^+ = 2HOBr \quad (A2)$$

$$HOBr + Br^- + H^+ = Br_2 + H_2O \quad (A3)$$

$$BrO_3^- + HBrO_2 + H^+ = 2BrO_2\cdot + H_2O \quad (B1)$$

$$BrO_2\cdot + Fe(II) + H^+ = HBrO_2 + Fe(III) \quad (B2)$$

$$2HBrO_2 = BrO_3^- + HOBr + H^+ \quad (B3)$$

Bromide, initially present in the reaction mixture, is slowly consumed by bromate oxidation in process A. Process B becomes dominant when bromide reaches a critical concentration, $[Br^-]_c$, and ferroin is oxidized to

(1) B. P. Belousov, *Ref. Radiats. Med.*, **1958**, 145 (1959).
(2) (a) A. M. Zhabotinsky, *Dokl. Akad. Nauk. SSSR*, **157**, 392 (1964); (b) A. N. Zaikin and A. M. Zhabotinsky, *Nature (London)*, **225**, 535 (1970).
(3) A. T. Winfree, *Science*, **175**, 634 (1972).
(4) R. J. Field and R. M. Noyes, *J. Am. Chem. Soc.*, **96**, 2001 (1974).
(5) R. J. Field, E. Körös, and R. M. Noyes, *J. Am. Chem. Soc.*, **94**, 8649 (1972).
(6) E. J. Reusser and R. J. Field, *J. Am. Chem. Soc.*, **101**, 1063 (1979).
(7) R. J. Field and R. M. Noyes, *J. Chem. Phys.*, **60**, 1877 (1974).
(8) K. Showalter, R. M. Noyes, and H. Turner, *J. Am. Chem. Soc.*, **101**, 7463 (1979).
(9) W. Geiseler and H. H. Föllner, *Biophys. Chem.*, **6**, 107 (1977).
(10) K. Bar-Eli and R. M. Noyes, *J. Phys. Chem.*, **82**, 1352 (1978).
(11) R. M. Noyes, *J. Chem. Phys.*, **72**, 3454 (1980).

(12) The term *trigger wave* was first introduced by Winfree in "Lecture Notes in Biomathematics", P. van den Dreische, Ed., Springer-Verlag, New York, 1974. We use the term interchangeably for waves in the BZ reaction and in the ferroin–bromate reaction because it seems particularly descriptive. It should be noted, however, that waves in an excitable BZ medium and waves in a ferroin–bromate reaction mixture may be distinguished by designating the former *pulses* and the latter *fronts* (see P. Ortoleva and J. Ross, *J. Chem. Phys.*, **60**, 5090 (1974)).
(13) R. J. Field, *J. Chem. Phys.*, **63**, 2289 (1975).
(14) K. Showalter, R. M. Noyes, and K. Bar-Eli, *J. Chem. Phys.*, **69**, 2514 (1978).

0022-3654/81/2085-0440$01.00/0

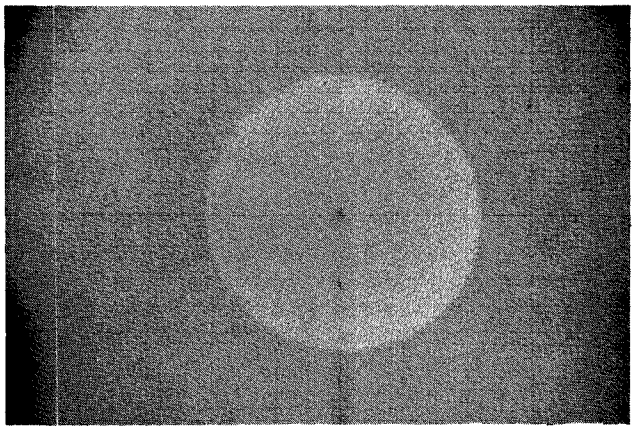

Figure 1. Trigger wave at 31.5 min initiated at ca. 11.5 min after mixing reactants. Solution composition in Table I except $[C_6H_8(COOH)_2] = 9.67 \times 10^{-2}$ M and $[KBr] = 6.70 \times 10^{-2}$ M. The field of view is ca. 6 cm × 10 cm.

ferriin in a reaction involving autocatalytic generation of $HBrO_2$. At the critical bromide concentration, the reaction mixture suddenly changes from orange (colored by ferroin) to blue (colored by ferriin). We refer to this change as the oxidation transition.

Prior to the oxidation transition, in an unstirred thin film of solution, a region can be switched from process A to process B by locally depleting bromide. Bromous acid, generated in the oxidized region, diffuses into surrounding regions in the reduced state. Bromide is consumed by bromous acid in reaction A2 until these surrounding regions are switched from process A to process B. The result is a propagating trigger wave. The rate of $HBrO_2$ autocatalysis is the dominant factor in wave propagation; however, the concentration of bromide in the reduced region ahead of the advancing wave, $[Br^-]_{red}$, is also important. When $[Br^-]_{red}$ is slightly greater than $[Br^-]_c$, bromous acid diffusing into the reduced region readily consumes bromide to the critical switching concentration. Wave propagation is possible when $[Br^-]_{red}$ is substantially greater than $[Br^-]_c$; however, a critical bromide concentration exists, $[Br^-]_{tw}$. When $[Br^-]_{red} \geq [Br^-]_{tw}$, wave propagation into the reduced region is inhibited.

Trigger waves were initiated before the bulk oxidation transition, in reaction mixtures in the reduced state. Elemental bromine is generated during process A dominance from reaction of Br^- with HOBr in (A3). The Br_2 reacts destructively with ferroin to form an insoluble brick-red substance. Addition of 4-cyclohexene-1,2-dicarboxylic acid, a water-soluble unsaturated compound that rapidly consumes Br_2, prevents formation of the precipitate. Our trigger wave studies utilized reaction mixtures containing $C_6H_8(COOH)_2$ in stoichiometric excess (see Results),[15] thus assuring a homogeneous reaction mixture.

Experimental Section

Materials and Equipment. Solutions were prepared with doubly distilled water and reagent grade chemicals with the exception of twice-recrystallized practical grade 4-cyclohexene-1,2-dicarboxylic acid. Concentrations of $NaBrO_3$, KBr, $Ce_2(SO_4)_3$, and ferroin solutions were determined by weight of dissolved chemical and concentrations of H_2SO_4 and 4-cyclohexene-1,2-dicarboxylic acid solutions were determined by titration with standardized base. Ferroin solution was prepared with $FeSO_4 \cdot 7H_2O$ and 1,10-phenanthroline in a 1:3 mole ratio. All solutions were filtered through 0.8-μm membrane filters before using.

Trigger wave studies were carried out by using a petri dish with an optically flat bottom, thermostated at 25.0 ± 0.2 °C by a water jacket. A Plexiglas cover, supported by the walls of the thermostated petri dish, prevented disturbance of the solution by air currents. The cover also served as a holder for the wave initiation and detection electrodes. A silver wire electrode (B & S Gauge No. 25) and a platinum wire electrode (B & S Gauge No. 26) were connected to a square wave generator for trigger wave initiation. The Ag electrode was negatively biased at −1.1 V except when a 3.0-V pulse of 30-ms duration was delivered. Trigger waves were detected by monitoring the potential difference between two platinum electrodes (B & S Gauge No. 26) in line of the advancing wave.

Measurements of bromide concentration in homogeneous solution were carried out with an Orion 901 Ionalyzer. The instrument was calibrated by using reaction mixtures containing all reactants except $NaBrO_3$.

Procedure. Solutions were prepared for each run by pipetting appropriate volumes of stock solutions. $NaBrO_3$ reagent was added last by rapid delivery pipet and complete delivery was defined as time zero. The solution was thoroughly mixed and spread uniformly into the dish, and electrodes were positioned. The solution volume of 21.0 mL generated a solution depth of 1.7 mm in the petri dish. To ensure trigger wave initiation before the bulk oxidation transition occurred, a positive voltage pulse was delivered 1.0 min after time zero and repeated every 30 s. A film of blue solution surrounding the silver electrode signaled the initiation of a wave. Pulses delivered after the blue film appeared had no effect on the initiated wave. Therefore, pulses were delivered until the blue film could be visually detected and were then discontinued. The initiated trigger wave was allowed to propagate through the Pt detection electrodes. For all determinations of wave velocity as a function of reactant concentrations, the detection electrodes were accurately positioned in line 3.0 and 6.0 mm from the Ag electrode. In these experiments, one reactant concentration was varied over the range shown in Table I and all other reactant concentrations were held constant.

TABLE I

reactant	concn/M	concn range/M
H_2SO_4	0.189	0.142-0.189
$NaBrO_3$	9.51×10^{-2}	$(6.66\text{-}11.4) \times 10^{-2}$
ferroin	1.21×10^{-3}	$(0.805\text{-}1.61) \times 10^{-3}$
KBr	4.79×10^{-2}	$(3.35\text{-}6.22) \times 10^{-2}$
$C_6H_8(COOH)_2$	8.97×10^{-2}	$(8.52\text{-}10.8) \times 10^{-2}$

Measurements of wave velocity as a function of time were made by using photographs taken at timed intervals. These experiments utilized the concentrations listed in Table I except $[KBr] = 6.22 \times 10^{-2}$ M and $[C_6H_8(COOH)_2] = 9.67 \times 10^{-2}$ M.

Results

Reaction Stoichiometry and Kinetics. Trigger wave studies utilized reaction mixtures containing 4-cyclohexene-1,2-dicarboxylic acid in stoichiometric excess to prevent formation of elemental bromine. Reaction stoi-

(15) Reaction mixtures containing Br^- in stoichiometric excess of $C_6H_8(COOH)_2$ according to (A') often developed mosaic spatial structures, depending on the quantity of Br_2 generated (see K. Showalter, *J. Chem. Phys.*, 73, 3735 (1980)). The pattern formation prevented uniform propagation of trigger waves and therefore all quantitative experiments were restricted to reaction mixtures containing $C_6H_8(COOH)_2$ in stoichiometric excess of Br^-. A reaction mixture containing stoichiometrically limiting $C_6H_8(COOH)_2$ was used for Figure 1 because that composition generated a particularly striking trigger wave. Trigger waves in the quantitative experiments developed only to ca. 1.0–1.6 cm in diameter before they were annihilated by the oxidation transition.

chiometry was determined by using stirred solutions containing stoichiometrically limiting $C_6H_8(COOH)_2$. In these reaction mixtures, a sudden change in the rate of bromide consumption occurred at the same time a brick-red colloidal substance suddenly appeared. The rate change and precipitation could be detected only if it occurred before the bulk oxidation transition. Independent qualitative experiments showed that direct reaction of ferroin with bromine water generates an insoluble brick-red substance identical in appearance with the precipitate.

The net chemical reaction for process A in reaction mixtures containing no $C_6H_8(COOH)_2$ is given by (A1) + (A2) + 3(A3) or (A).[5] Bromination of unsaturated compounds in aqueous solution may generate either the bromohydrin or dibromide product, the latter being favored by high Br^- concentration.[16] Bromination of $C_6H_8(COOH)_2$ to form the bromohydrin is given by (A4).

$$BrO_3^- + 5Br^- + 6H^+ = 3Br_2 + 3H_2O \quad (A)$$

$$Br_2 + C_6H_8(COOH)_2 + H_2O = C_6H_8(Br)(OH)(COOH)_2 + Br^- + H^+ \quad (A4)$$

The net reaction for process A in reaction mixtures containing excess $C_6H_8(COOH)_2$ is given by (A1) + (A2) + 3(A3) + 3(A4) or (A′), if the bromohydrin is generated.

$$BrO_3^- + 2Br^- + 3H^+ + 3C_6H_8(COOH)_2 = 3C_6H_8(Br)(OH)(COOH)_2 \quad (A')$$

Direct attack of HOBr on $C_6H_8(COOH)_2$ generates an identical stoichiometry. An experiment was conducted to determine the reaction stoichiometry by monitoring $[Br^-]$ as a function of time in a stirred reaction mixture (composition in Table I except $[Br^-] = 4.79 \times 10^{-2}$ M and $[C_6H_8(COOH)_2] = 6.90 \times 10^{-2}$ M). At the time when the rate acceleration occurred, the ratio of consumed Br^- to initial $C_6H_8(COOH)_2$ was 2.000:2.949, almost exactly that predicted by (A′).

Pseudo-first-order rate constants for the consumption of bromide were determined for times before and after the $C_6H_8(COOH)_2$ stoichiometric point. Reaction mixtures suitable for trigger wave experiments contained H^+ and BrO_3^- in 2–3-fold excess over Br^- according to the stoichiometry of (A′). Rate constants derived from $[Br^-]$ vs. time data were only approximately pseudo-first order because H^+ and BrO_3^- were significantly depleted during a run; however, first-order Guggenheim[17] treatments generated reasonably linear plots. The stoichiometry experiment above was utilized to determine apparent rate constants. The constants, evaluated for times before and after the $C_6H_8(COOH)_2$ stoichiometric point, are $k_\alpha = 2.26 \times 10^{-2}$ s^{-1} and $k_\Omega = 1.78 \times 10^{-2}$ s^{-1}, respectively.

Assuming that Br_2 consumption by (A4) is rapid compared to the rate limiting step for its production, (A1),[5] the apparent rate constants are given by eq 1, where γ is

$$k_{\alpha,\Omega} = \gamma k_{A1}[BrO_3^-][H^+]^2 \quad (1)$$

a stoichiometric factor of 2 for k_α and 5 for k_Ω. Values of γk_{A1} were calculated from k_α by using the initial $[H^+]$ and $[BrO_3^-]$ and from k_Ω by using the concentrations predicted by (A′) after consumption of $C_6H_8(COOH)_2$. The ratio $(\gamma k_{A1})_\Omega/(\gamma k_{A1})_\alpha$ evaluated in this manner is 2.42, in good agreement with that expected from stoichiometry. Values of k_α and k_Ω, calculated from the literature value of k_{A1}[5] and the appropriate $[H^+]$ and $[BrO_3^-]$, are 1.60×10^{-2} and 1.30×10^{-2} s^{-1}, respectively. The calculated values are lower than the experimental values by a factor of 0.7.

(16) J. R. Atkinson and R. P. Bell, *J. Chem. Soc.*, 3260 (1963).
(17) E. A. Guggenheim, *Phil. Mag.*, 2, 538 (1926).

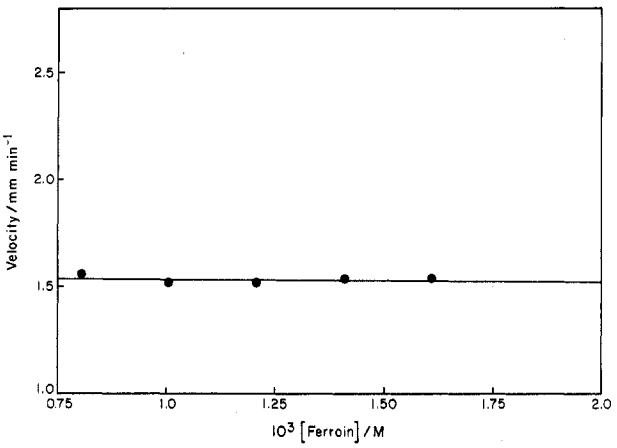

Figure 2. Trigger wave velocity as a function of [ferroin]. Solution composition in Table I.

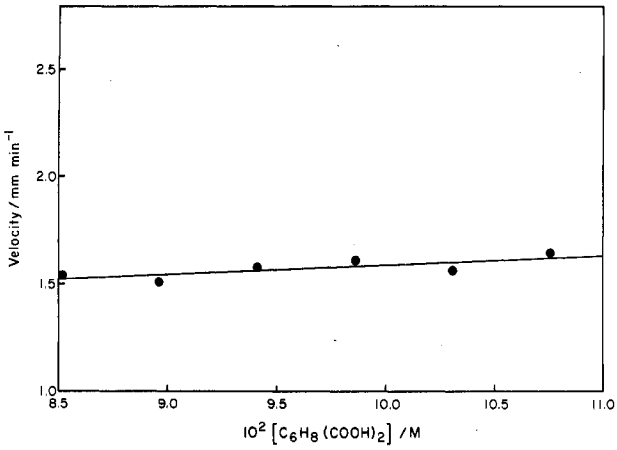

Figure 3. Trigger wave velocity as a function of $[C_6H_8(COOH)_2]$. Solution composition in Table I.

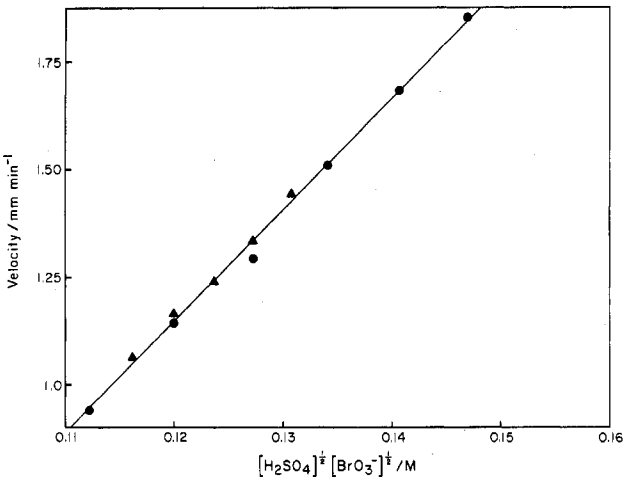

Figure 4. Trigger wave velocity as a function of $[H_2SO_4]^{1/2}[BrO_3^-]^{1/2}$. Solution composition in Table I. Circles are for BrO_3^- series and triangles are for H_2SO_4 series.

Effect of Reactant Concentrations on Wave Propagation. Five series of experiments were conducted to determine the effect of reactant concentrations on trigger wave velocity. In each series, one reactant was varied over a range and the other reactants were held constant (concentrations listed in Table I). The wave initiation time and the time that the bulk oxidation transition occurred were functions of reactant concentrations. The experiment

TABLE II

$10^2[Br^-]$/ M	velocity/ mm min^{-1}	$10^2[Br^-]$/ M	velocity/ mm min^{-1}
3.35	2.22	5.26	1.43
3.83	1.83	5.74	1.31
4.31	1.57	6.22	1.30
4.79	1.51		

required sufficient time between wave initiation and bulk oxidation transition for wave propagation through the detection electrodes. This time factor limited the concentration ranges to those listed in Table I.

Wave velocity dependence on initial reactant concentrations is shown in Figures 2–4. Figures 2 and 3 show that [ferroin] and $[C_6H_8(COOH)_2]$ have little effect on wave velocity. A linear dependence of wave velocity on the product $[H_2SO_4]^{1/2}[BrO_3^-]^{1/2}$ is shown in Figure 4. Field and Noyes[4] demonstrated that trigger wave propagation in the BZ reaction depends primarily on the autocatalytic generation of $HBrO_2$. A reaction-diffusion equation including only (B1), the rate-determining step for the autocatalysis, predicts wave velocity to be a function of the above product. A linear least-squares fit of the data in Figure 4 gives eq 2, in excellent agreement with the experimental velocity dependence found in the BZ reaction.[4]

$$\nu/\text{mm min}^{-1} = -1.957 + 25.86[H_2SO_4]^{1/2}[BrO_3^-]^{1/2}/\text{M} \quad (2)$$

Initial $[Br^-]$ was varied in one series of experiments. The velocity dependence in these experiments was complicated by significant consumption of H^+ and BrO_3^- by the time wave velocities could be measured. Bromide concentration was ca. 5.4×10^{-5} M when wave initiation became possible (see Critical Bromide Concentrations), leaving less than 0.2% of that initially present. The variation of initial $[Br^-]$ results in a corresponding variation in $[H^+]$ and $[BrO_3^-]$ at the time of wave initiation. Wave velocities as a function of initial $[Br^-]$, given in Table II, therefore reflect velocity dependence on H^+ and BrO_3^- and are not due solely to $[Br^-]$. The constant initial $[Br^-]$ in the other experiments ensured that $[H^+]$ and $[BrO_3^-]$ at the time of wave initiation reflected the initial values.[18]

Effect of Reactant Concentrations on Wave Initiation. Repeated application of positive voltage pulses to the Ag electrode guaranteed wave initiation as soon as the medium would allow. Approximate initiation times were indicated by the appearance of a blue film of solution surrounding the Ag electrode. These times, however, were not of sufficient accuracy to determine the dependence of wave initiation time on initial reactant concentrations. Initiation times were obtained indirectly from the average times of detection at the Pt electrodes, available from the wave velocity experiments. For each experiment, the initiation time was calculated by extrapolating the time of wave detection to the time of zero propagation, using the measured wave velocity. Wave velocity was assumed to be independent of time in each calculation. Wave velocity is not constant (see Trigger Wave Velocity); however, its variation is slight. These extrapolated initiation times are subsequently referred to as β values.

The dependence of β on initial reactant concentrations can be related to the consumption of Br^-, for which reaction A1 is rate determining.[5] An approximately pseudo-first-order consumption of Br^- to a critical concentration $[Br^-]_{tw}$, at which trigger wave initiation becomes possible, is indicated by the relationships shown in Figures 5–7. Initial concentrations of $C_6H_8(COOH)_2$ and ferroin had little effect on initiation times and are not shown.

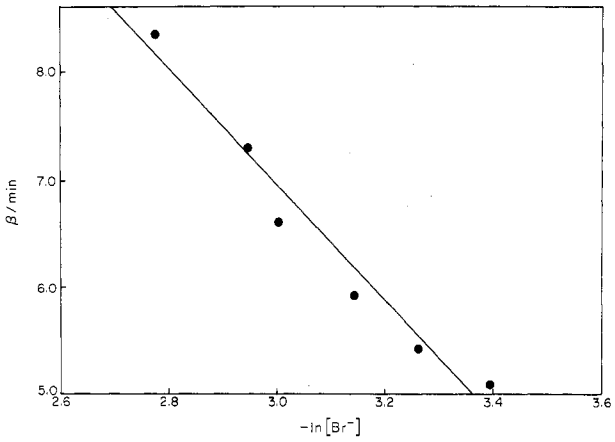

Figure 5. Wave initiation time β as a function of $-\ln [Br^-]$. Solution composition in Table I.

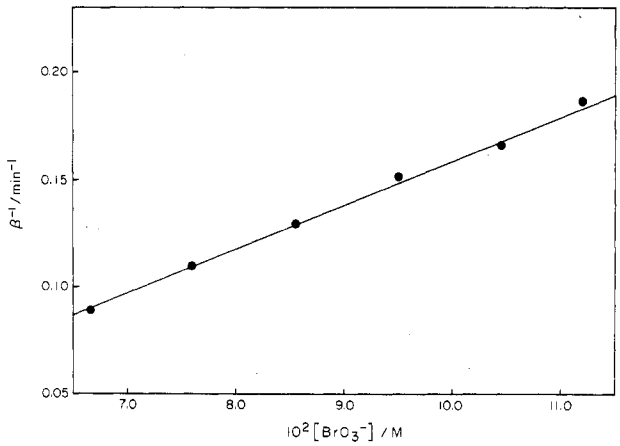

Figure 6. Reciprocal wave initiation time β^{-1} as a function of $[BrO_3^-]$. Solution composition in Table I.

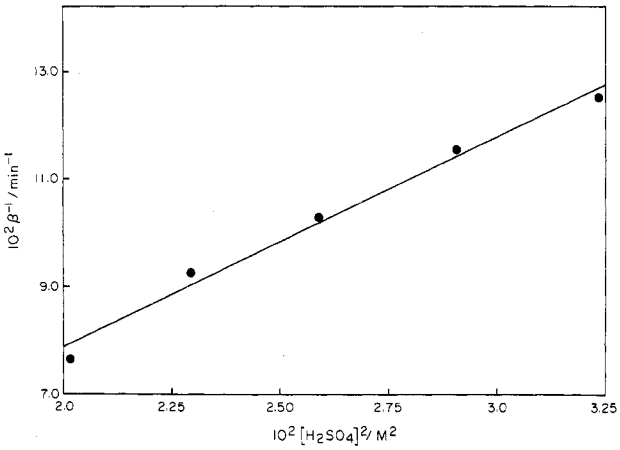

Figure 7. Reciprocal wave initiation time β^{-1} as a function of $[H_2SO_4]^2$. Solution composition in Table I.

(18) Initial concentrations were used to calculate $[H_2SO_4]^{1/2}[BrO_3^-]^{1/2}$ in Figure 4 and therefore ν in eq 2 is a function of initial concentrations. Wave velocity as a function of H_2SO_4 and BrO_3^- concentrations at the time of wave initiation was determined by assigning $[Br^-]_{tw}$ a value of 5.4×10^{-5} M (see Critical Bromide Concentrations) and correcting H_2SO_4 and BrO_3^- concentrations for the consumption of initial bromide to $[Br^-]_{tw}$. A plot of ν vs. $[H_2SO_4]^{1/2}[BrO_3^-]^{1/2}$ with the corrected concentrations is reasonably linear and a least-squares fit of the data gives

$$\nu/\text{mm min}^{-1} = -0.999 + 27.33[H_2SO_4]^{1/2}[BrO_3^-]^{1/2}/\text{M}$$

in excellent agreement with the velocity dependence found in the BZ reaction.[4]

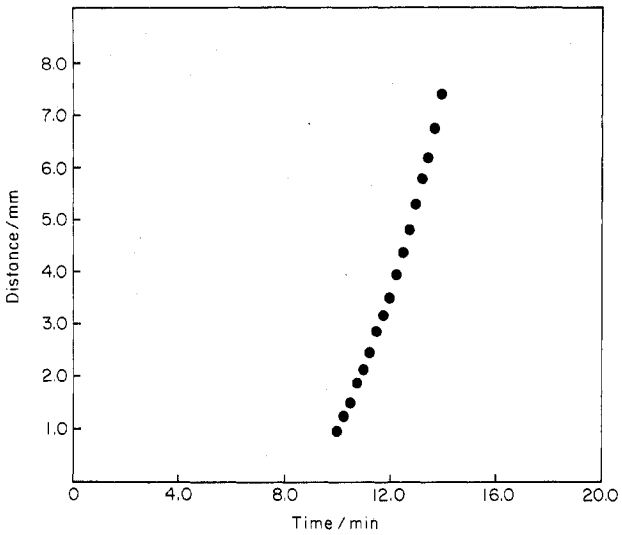

Figure 8. Wave front position as a function of time. Solution composition in Table I except [KBr] = 6.22×10^{-2} M and $[C_6H_8(COOH)_2] = 9.67 \times 10^{-2}$ M.

Figure 5 shows a plot of β vs. ln $[Br^-]$, where initial $[Br^-]$ was varied over the range in Table I. Bromide is consumed to $[Br^-]_{tw}$ in time β according to (3). The value of $[Br^-]_{tw}$

$$\ln ([Br^-]/[Br^-]_{tw}) = (k_{app})\beta = 2k_{A1}[H_2SO_4]^2[BrO_3^-]\beta \quad (3)$$

is probably a function of initial concentrations; however, its variation should be small compared to the variation in initial bromide concentration. Assigning $[Br^-]_{tw}$ a constant value of 5.4×10^{-5} M (see Critical Bromide Concentrations) allows a comparison to be made between the literature value of k_{A1} and that calculated from (3). The least-squares slope of ln $[Br^-]$ vs. β is 0.18 min^{-1}. The value of k_{A1} calculated by using the slope k_{app} and corrected concentrations of H_2SO_4 and BrO_3^- is 1.51 M^{-3} s^{-1}, compared to the literature value of 2.1 M^{-3} s^{-1}.[5] The concentrations of H_2SO_4 and BrO_3^- were corrected to approximate those at the time of wave initiation by assuming the reaction of 4.79×10^{-2} M Br^-, the mean bromide concentration in Figure 5.

For a constant initial $[Br^-]$, the β values are inversely related to $[BrO_3^-]$ and $[H_2SO_4]^2$, because the term ln $([Br^-]/[Br^-]_{tw})$ in (3) becomes a constant. A plot of β^{-1} vs. $[BrO_3^-]$ is shown in Figure 6 (composition in Table I with $[BrO_3^-]$ varied). A similar plot of β^{-1} vs. $[H_2SO_4]^2$ is shown in Figure 7 (composition in Table I with $[H_2SO_4]$ varied). Experimental values of k_{A1} were calculated with (3) by assigning $[Br^-]_{tw} = 5.4 \times 10^{-5}$ M and correcting H_2SO_4 and BrO_3^- concentrations for the consumption of initial bromide to $[Br^-]_{tw}$. The values of k_{A1} calculated from the BrO_3^- series and H_2SO_4 series are 8.32 and 5.59 M^{-3} s^{-1}, respectively.

Trigger Wave Velocity. Experiments were conducted with trigger wave propagation monitored photographically as a function of time. Wave front position vs. time was determined by averaging orthogonal diameters of oxidized region and dividing by 2. Accuracy of the measurements was enhanced by projecting 35-mm slides, thereby enlarging the photographic image. The time record of wave front position is shown in Figure 8 (composition in Table I except $[Br^-] = 6.22 \times 10^{-2}$ M and $[C_6H_8(COOH)_2] = 9.67 \times 10^{-2}$ M). A blue film of solution surrounding the Ag electrode, signaling initiation of the wave, appeared at 9.0 min; however, accurate diameter measurements were not possible until the wave had advanced ca. 1.0 mm.

Figure 8 shows that the wave accelerates from the time of initiation until it is annihilated by the oxidation transition at 14.2 min. At least-squares program for fitting power curves was used to fit the data. The curve given by (4), where $a = 1.53 \times 10^{-4}$ mm s^{-b} and $b = 1.83$, is in

$$x = a(t)^b \quad (4)$$

excellent agreement with the curve defined by the experimental points (coefficient of determination $r^2 = 0.998$).[19a] In this calculation, 8.0 min was defined as time zero. Extrapolation of (4) to a distance corresponding to the radius of the Ag electrode (0.25 mm) gives a wave initiation time of 9.1 min, in good agreement with the qualitative determination. The time derivative of (4) gives $v/\text{mm s}^{-1} = 2.80 \times 10^{-4}(t)^{0.83}$, indicating that velocity increases almost linearly with time.

An attempt was made to correlate wave velocity to $[Br^-]_{red}$ by determining $[Br^-]$ as a function of time in a stirred reaction mixture with the same composition. Treatment of the $[Br^-]$ vs. time data between 8.3 and 14.2 min with the Guggenheim method[17] for first-order reactions produced a good straight line ($r^2 = 0.997$),[19b] generating the apparent first-order rate constant $k_{app} = 8.97 \times 10^{-3}$ s^{-1}. The pseudo-first-order consumption of Br^- in the stirred solution indicates that while wave velocity increases almost linearly with time, $[Br^-]_{red}$ decreases logarithmically. An inverse relation between wave velocity and $[Br^-]_{red}$ would be expected if velocity increased exponentially with time. A program for fitting exponential curves was used with the data in Figure 8, generating the curve $x = (1.21$ mm) $\exp(8.09 \times 10^{-3}$ $s^{-1})(t)$. In this calculation, 10.0 min was defined as time zero. The agreement between this curve and the experimental points is only fair ($r^2 = 0.970$).[19c] Extrapolation of the calculated curve to a distance corresponding to the radius of the Ag electrode gives a wave initiation time of 6.75 min, about 2 min earlier than the qualitative determination.

Critical Bromide Concentrations. Trigger wave initiation time was visually determined in the wave velocity experiment, defined by the first appearance of a blue film of solution surrounding the Ag electrode. The initiation time in this experiment was 9.0 min (see Trigger Wave Velocity). The critical bromide concentration for wave initiation, $[Br^-]_{tw} = 5.4 \times 10^{-5}$ M, was determined by correlating the initiation time with $[Br^-]$ vs. time data. The same experiment allowed determination of the critical

(19) (a)

$$r^2 = \frac{\left[\sum(\ln t_i)(\ln x_i) - \frac{(\sum \ln t_i)(\sum \ln x_i)}{n}\right]^2}{\left[\sum(\ln t_i)^2 - \frac{(\sum \ln t_i)^2}{n}\right]\left[\sum (\ln x_i)^2 - \frac{(\sum \ln x_i)^2}{n}\right]}$$

where x = distance/mm and t = time/s. (b)

$$r^2 = \frac{\left[\sum t_i x_i - \frac{\sum t_i \sum x_i}{n}\right]^2}{\left[\sum t_i^2 - \frac{(\sum t_i)^2}{n}\right]\left[\sum x_i^2 - \frac{(\sum x_i)^2}{n}\right]}$$

where $x = \ln ([Br^-]_t - [Br^-]_{t+\tau})$, t = time/s, and $\tau = 120$ s. (c)

$$r^2 = \frac{[\sum t_i \ln x_i - (1/n)\sum t_i \sum \ln x_i]^2}{\left[\sum t_i^2 - \frac{(\sum t_i)^2}{n}\right]\left[\sum (\ln x_i)^2 - \frac{(\sum \ln x_i)^2}{n}\right]}$$

where x = distance/mm and t = time/s.

bromide concentration for the bulk oxidation transition, $[Br^-]_c$. The bromide electrode measurements, calibrated to correct for the nonlinear response at low concentration, showed that for this reaction mixture $[Br^-]_c = 5 \times 10^{-7}$ M, comparing favorably with that predicted by the FKN mechanism ($[Br^-]_c = (k_{B1}/k_{A2})[BrO_3^-] = 3.1 \times 10^{-7}$ M).[5] These experiments demonstrate that $[Br^-]_{tw}$ is greater than $[Br^-]_c$ by about two orders of magnitude for this particular reaction mixture. The value of $[Br^-]_{tw}$ is probably a function of reactant concentrations, however, its concentration dependence was not determined in this study.

Effect of Metal Ion Catalyst. Experiments were conducted to investigate trigger wave initiation and propagation in reaction mixtures containing Ce(III) in place of ferroin as the metal ion catalyst. Two experiments were conducted (composition in Table I except [Ce(III)] = 1.21 $\times 10^{-3}$ M) which demonstrated that trigger waves similar to those in reaction mixtures containing ferroin could be initiated; however, the waves were not visually detectable with the low concentration of cerium. The average wave velocity, determined by using Pt detection electrodes, was about 18% greater with Ce(III) than with ferroin in otherwise identical experiments.

Discussion

The oxidation of various weak one-electron reducing agents by acidic bromate gives rise to a variety of unusual chemical phenomena. The relatively simple bromate chemistry forms the basis of a number of oscillating reactions, most notably the BZ reaction. Noyes[20] has recently unified the various bromate oscillators in terms of FKN bromate chemistry. The reaction sequence (A1)–(B3), a distillation of FKN bromate chemistry, is a minor modification of Field's reversible Oregonator,[13] an extension of the original Oregonator by Field and Noyes.[7]

Trigger waves, first discovered in the BZ reaction[2b] and now known in the uncatalyzed bromate oscillators[21] and in the ferroin-bromate system reported here, represent a particularly intriguing kinetic behavior of bromate chemistry. Two coupled reaction pathways, one involving rapid autocatalysis and the other a slow consumption of a reactant that inhibits autocatalysis, make bromate systems kinetically ideal for displaying trigger wave behavior. In the ferroin–bromate system, the propagating wave consumes reduced solution leaving behind oxidized solution, thus partitioning the reaction mixture into two very different kinetic states.

Our study of ferroin–bromate trigger wave behavior provides strong support for the Field–Noyes[4] mechanism of trigger wave propagation in the BZ reaction. The experimentally determined wave velocity dependence on the product $([BrO_3^-][H_2SO_4])^{1/2}$ is almost identical in the two systems. The absence of a velocity dependence on ferroin or the organic material is also very similar in the two systems. The autocatalytic generation of $HBrO_2$ is clearly the dominant factor in wave propagation in the bromate systems.

The wave velocity dependence on $[Br^-]$ is difficult to determine in the BZ reaction. Regeneration of Br^- by metal ion oxidation of bromomalonic acid is affected by atmospheric oxygen; therefore $[Br^-]$ in the reduced solution ahead of an advancing wave depends on the extent of air saturation.[8] The model calculations of BZ trigger waves by Reusser and Field[6] indicated that wave velocity is inversely proportional to $[Br^-]_{red}$. An inverse dependence has also been found in other theoretical studies based on the FKN mechanism.[22] The correlation of wave velocity from Figure 8 with independent $[Br^-]$ vs. time measurements suggests that the velocity dependence on $[Br^-]_{red}$ may be more complicated than a simple inverse relationship.

Calculated wave velocities in the BZ reaction derived by considering only the autocatalytic generation of $HBrO_2$ are higher than experimental velocities by about a factor of 20.[4] Reaction of $HBrO_2$ with Br^- in (A2) has been used to explain the discrepancy.[23] An expression for wave velocity derived from a reaction-diffusion equation including both reactions (B1) and (A2) is given by eq 5. This expression is valid for a region within the wave front, and adjustment of $[Br^-]$ generates a velocity matching experiment.[23] The appropriate $[Br^-]$ is slightly less than $[Br^-]_c$, suggesting that (5) pertains to a region in the wave front slightly behind the point where the rates of reactions B1 and A2 become equal. We were unable to relate the velocity dependence on $[Br^-]_{red}$ suggested by (4) to the dependence on $[Br^-]$ within the wave given by (5).

$$v = \{4D(k_{B1}[H^+][BrO_3^-] - k_{A2}[H^+][Br^-])\}^{1/2} \quad (5)$$

A kinetic behavior of bromate chemistry especially relevant to the reaction-diffusion behavior in the ferroin–bromate system is the kinetic bistability exhibited in the acidic bromate oxidation of Ce(III) in a CSTR.[9] For a range of reactor residence times (reactor volume divided by flow rate), the chemical system may exist in two very different kinetic states. The elemental composition of the reaction mixture at any particular residence time is invariant; however, the concentrations of molecular and ionic species making up the reaction intermediates differ by orders of magnitude in the two kinetic states. The physically realizable stationary states are stable to infinitesimal perturbation. These states are separated by an unstable stationary state. When the concentration of a critical intermediate species such as Br^- is perturbed a finite amount, a transition from one stable state to the other may occur. Bar-Eli and Noyes[10] have accounted for the bistability behavior almost quantitatively with numerical simulations based on FKN bromate chemistry.

The trigger wave behavior in the ferroin–bromate system represents another mode of kinetic bistability. Local depletion of Br^- in the reduced state nucleates a region in the oxidized state that grows as a propagating front. The single reaction mixture becomes differentiated into two very different kinetic states, the oxidized state behind the front and the reduced state ahead. Of course, the states are not true stationary states as in the CSTR experiment because the reaction-diffusion experiment must utilize a closed system.

Noyes[11] has recently developed a reduced model of the Ce(III)–bromate reaction for examining relative "dynamic stabilities" of kinetic states. The model is given by the reaction sequence N1–N4. Reaction N1 and N2 represent

$$A + Y \rightarrow X + P \quad (N1)$$

$$X + Y \rightarrow 2P \quad (N2)$$

$$A + X \rightarrow 2X \quad (N3)$$

$$2X \rightarrow A + P \quad (N4)$$

reactions A1–A3, or process A, and reactions N3 and N4 represent reactions B1–B3, or process B. The corresponding species are identified as $A = BrO_3^-$, $X = HBrO_2$,

(20) R. M. Noyes, *J. Am. Chem. Soc.*, **102**, 4644 (1980).
(21) M. Orbán, *J. Am. Chem. Soc.*, **102**, 4311 (1980).
(22) (a) J. D. Murray, *J. Theor. Biol.*, **56**, 329 (1976); (b) S. Schmidt and P. Ortoleva, *J. Chem. Phys.*, **72**, 2733 (1980).
(23) J. Tilden, *J. Chem. Phys.*, **60**, 3349 (1974).

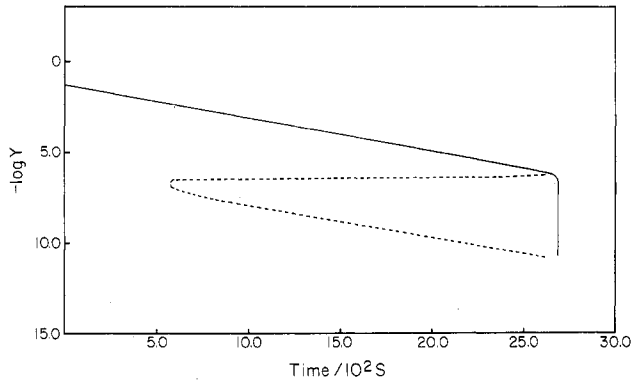

Figure 9. Bromide ion concentration (Y) as a function of time according to reactions N1–N4. At $t = 0$, $Y = 4.786 \times 10^{-2}$ M, $X = 1.0 \times 10^{-10}$ M, and $A = 7.117 \times 10^{-2}$ M. The concentration of A was held constant. $k_{N1} = 2.904 \times 10^{-2}$ M^{-1} s^{-1}, $k_{N2} = 2.35 \times 10^{8}$ M^{-1} s^{-1}, $k_{N3} = 1.176 \times 10^{3}$ M^{-1} s^{-1}, and $k_{N4} = 4.0 \times 10^{7}$ M^{-1} s^{-1}. See text for explanation of dashed line.

Y = Br^-, and P = HOBr. Hydrogen ion concentration is considered constant and is therefore absorbed into the rate constants. Step A3 is unimportant to the kinetic behavior of process A and is omitted in the model. The kinetic behavior of process B is determined primarily by the rate-limiting step for autocatalysis (B1) and the bimolecular termination step (B3). Therefore, the kinetic features of process B are retained without explicitly including the metal ion in step B2.

The solid line in Figure 9 shows the pseudo-first-order consumption of bromide ion (Y) in batch reaction according to model N. In this calculation,[24] the model was reduced to two variables, X and Y, by holding A constant.[25] After bromide is consumed to its critical concentration ($Y = 3.6 \times 10^{-7}$ M) at 2689 s, it is rapidly depleted by reaction with autocatalytically generated bromous acid (X) in (N2). Irreversibility in the model results in Y being driven to zero concentration at 2689.45 s. The initial bromide concentration in the calculation corresponds to the composition in Table I. The fixed values of $[H^+]$ and $[BrO_3^-]$, however, were adjusted to correspond to the solution composition when $[Br^-] = [Br^-]_{tw}$.

Even as a two-variable model, reactions N1–N4 faithfully reproduce the qualitative features of bistability in the cerium(III)–bromate system.[11] We used model N to help explain "spatial bistability" in the ferroin–bromate trigger wave experiment. The experiment demonstrates that perturbation-induced transitions from state A (process A dominance) to state B (process B dominance) are possible and that both states may exist simultaneously for a period of time. Similar state A → state B transitions should be possible in homogeneous batch reaction with an appropriate perturbation, such as injection of $AgNO_3$ solution. Conceptual difficulties are encountered in modeling, however, because Br^- (Y) is only consumed in reactions N1–N4 and therefore never attains even a pseudostationary state.

Bromide concentration changes slowly during the long induction period and can be considered constant in a vanishingly small time increment. If $[Br^-]$ is maintained constant in that time increment by introducing a source of Br^- entering at an appropriate rate, then model N can be used to investigate the existence of multiple kinetic states. The kinetic equations generated by model N containing the bromide source k_0Y_0 are

$$dX/dt = k_1AY - k_2XY + k_3AX - 2k_4X^2 \quad (6)$$

$$dY/dt = k_0Y_0 - k_1AY - k_2XY \quad (7)$$

Equations 6 and 7 were used to solve for the bromide source, k_0Y_0, necessary to maintain steady-state concentrations of X and Y at a particular instant. Values of k_0Y_0 were obtained for each value of Y on the solid line in Figure 9. The k_0Y_0 values were then used to solve for the corresponding steady-state concentrations of Y at each instant. For every value of k_0Y_0 between 575 and 2643 s, three positive real roots were generated by the cubic equation. Of course, one root simply regenerated the solid line between these times. The other two roots are represented by the dashed lines. Linear stability analyses demonstrated that the states on the lower dashed line and on the solid line are stable to infinitesimal perturbation. The states represented by the upper dashed line are unstable to infinitesimal perturbation. The unstable state remains at an almost constant concentration, increasing by less than a factor of 2, between 590 and 2600 s. The stable states are virtually parallel, with slopes determined by the pseudo-first-order consumption of Br^-.

The diagram in Figure 9 is useful for visualizing transitions between kinetic states in batch reaction. The blue oxidized state (state B) underlying the orange reduced state (state A) is not observed in the typical batch experiment because it is not ordinarily accessible. In the CSTR experiment, the hysteresis loop defining the bistability region can be mapped by simply scanning the flow rate. In the batch experiment, change in the reaction mixture composition occurs by chemical reaction and is of course unidirectional. However, the underlying oxidized state is accessible by a perturbation-induced transition, experimentally demonstrated by the initiation of trigger waves.

Noyes used model N to examine the relative "dynamic stabilities" of the stable stationary states in the CSTR experiment.[11] Two tanks identically pumped, one in state A and the other in state B, are allowed to mix. The pumping rate at which either state is equally likely to dominate upon mixing defines the states with equal "dynamic stability". The states are not unique, however, because different mixing rates generate different states of equal stability.

The reaction-diffusion experiment offers another approach for examining state stability. Bromide must be consumed to a critical concentration, $[Br^-]_{tw}$, before trigger wave initiation becomes possible. Wave velocity is zero at $[Br^-]_{tw}$, and as bromide is further consumed the wave accelerates according to Figure 8. Wave propagation in the reverse direction (orange into blue) would be expected when $[Br^-]_{red} > [Br^-]_{tw}$, although the wave would not be the same as the typical trigger wave observed when $[Br^-]_{red} < [Br^-]_{tw}$. Reverse propagation would occur by inward diffusion of Br^- from the bulk reduced solution, causing the oxidized solution in state B to be switched to state A.[26] Therefore, in a hypothetical reaction-diffusion experiment where the reaction mixture is maintained at the composition corresponding to $[Br^-]_{tw}$, an existing region of oxi-

(24) A. C. Hindmarsh, "Gear: Ordinary Differential Equation Solver", UCID-30001, Rev. 3, Dec 1974.

(25) The variable P does not appear in the kinetic equations because reactions (N1)–(N4) are irreversible.

(26) Diffusion of Br^- into a region of oxidized solution will switch off the $HBrO_2$ autocatalysis of state B, however, the affected region will not change from blue to orange unless ferriin is reduced. In the experiments reported here, the regeneration of ferroin might occur with the oxidation of $C_6H_8(COOH)_2$ (or the bromohydrin product) by ferriin attack at one of the tertiary hydrogens. If the rate of ferriin reduction by this reaction is too slow for a reasonable rate of reverse wave propagation, presumably a more suitable substrate could be introduced.

dation would have zero propagation velocity, and states A and B would coexist indefinitely. The compositions of state A and state B corresponding to the coexistence condition, $[Br^-]_{red} = [Br^-]_{tw}$, define states of equal "dynamic stability". This equal stability applies for mixing of states by the reaction-diffusion process and is no more unique than the states of equal stability defined by mixing the contents of two tank reactors.

Acknowledgment. We are grateful to the donors of the Petroleum Research Fund, administered by the American Chemical Society, and the West Virginia University Senate for support of this research. The capable technical assistance of Sharon E. Pritchard is gratefully acknowledged.

In Situ Photoacoustic Spectroscopy of Thin Oxide Layers on Metal Electrodes. Copper in Alkaline Solution

Ulrich Sander, Hans-Henning Strehblow,† and Jürgen K. Dohrmann*

Institut für Physikalische Chemie der Freien Universität Berlin, D-1000 Berlin 33, Federal Republic of Germany *(Received: May 9, 1980)*

A double-beam photoacoustic spectrometer is described for in situ studies of electrode processes. The electrochemical formation and reduction of oxide layers on copper (Cu_2O, CuO and/or $Cu(OH)_2$ of a thickness of <4 nm) has been monitored by in situ photoacoustic spectroscopy (PAS). The photoacoustic spectra of pure bulk copper and of the oxide-covered copper electrode in contact with 0.1 M KOH as well as the corresponding difference spectra are given and discussed. The photoacoustic signals at constant wavelength are closely related to the current density–potential curve. The PAS electrode-potential curves taken at 400 and 600 nm are significantly different and reflect the spectral characteristics attributed to Cu_2O and to Cu_2O/CuO, $Cu(OH)_2$ layers.

Introduction

Intermittent illumination of a light-absorbing sample enclosed in a gas-filled cell gives rise to the photoacoustic effect.[1] When radiationless processes contribute to the depopulation of excited states of the sample, heat is generated at and near the surface which, in turn, causes periodic fluctuations of the pressure in the surrounding gas. These can be measured by a microphone. The theory of the effect has been worked out.[2,3] Under certain conditions, the photoacoustic spectrum closely resembles the absorption spectrum of the material.

Presently, photoacoustic spectroscopy (PAS) is rapidly expanding as a tool in analytical chemistry.[4] Since photoacoustic spectra can be obtained easily and without the need of special sample preparation, PAS has some advantages in the spectroscopy of opaque and light-scattering samples where the use of absorption and reflection techniques is restricted. We therefore decided to examine whether PAS can be applied to the in situ study of the electrode/electrolyte interface simultaneously with electrochemical measurements. If so, it was hoped that PAS would provide information on the optical absorption of surface layers hitherto usually obtained by reflection spectroscopy[5] or ellipsometry.[6]

In this paper, we report the result of an in situ PAS study of thin (<4 nm) oxide layers on copper in contact with aqueous potassium hydroxide solution. Copper was chosen because the properties of the oxide layers have been thoroughly studied by electrochemical and other methods.[7] We use a cell assembly with the microphone located at the rear side of the working electrode (a copper foil) immersed in the electrolyte. A PAS technique similar to ours has been used independently by others for the study of solid/gas[8] and solid/electrolyte[9] interfaces. Very recently, a piezoelectric detector instead of a microphone has been employed to monitor the electrochemical formation of thick (>30 nm) precipitation layers on electrodes.[10]

Experimental Section

Figure 1 shows the block diagram of the double-beam photoacoustic spectrometer built for the present study. The light source is a 450-W high-pressure xenon arc (Osram XBO 450 W1) inside a closed lamp housing which uses an elliptical reflector and has an f number of 2.5 (Photochemical Research Associates, ALH 220). A stabilized power supply (Photochemical Research Associates, M 301) operates the lamp. The elliptical reflector focuses the arc onto the entrance slit of the monochromator (Jobin Yvon Model HL, aperture $f/2$, grating blazed at 300 nm). The light beam is interrupted by a mechanical chopper (Ortec-Brookdeal, 9479). The monochromatic light (band-pass of typically 10 nm) passes an order sorting filter and is focused by two quartz lenses onto the photoacoustic cell, A, containing the electrode under test. A quartz plate in the parallel beam serves as a beam splitter. Ca. 7% of the light is reflected at an angle of 30° with respect to the incident beam and provides the reference beam which is focused by another quartz lens onto the photoacoustic reference cell, B, containing a carbon powder sample. Cell B is similar to that described in ref 11. The PAS signal

†Institut für Physikalische Chemie II, Universität Düsseldorf, D-4000 Düsseldorf 1, Federal Republic of Germany

(1) A. G. Bell, *Philos. Mag.*, 11, 510 (1881).
(2) A. Rosencwaig and A. Gersho, *J. Appl. Phys.*, 47, 64 (1976).
(3) A. Rosencwaig in "Optoacoustic Spectroscopy and Detection", Yoh-Han Pao, Ed., Academic Press, New York, 1977, Chapter 8.
(4) R. B. Somoano, *Angew. Chem.*, 90, 250 (1978).
(5) J. D. E. McIntyre, *Adv. Electrochem. Electrochem. Eng.*, 9, 61 (1973).
(6) J. Kruger, Adv. *Electrochem. Electrochem. Eng.*, 9, 227 (1973).
(7) H.-H. Strehblow and B. Titze, *Electrochim. Acta*, 25, 839 (1980). See also the references therein.
(8) S. O. Kanstad and P. E. Nordal, *Infrared Phys.*, 19, 413 (1979).
(9) A. Fujishima, H. Masuda, and K. Honda, *Chem. Lett.*, 1063 (1979).
(10) R. E. Malpas and A. J. Bard, *Anal. Chem.*, 52, 109 (1980).

0022-3654/81/2085-0447$01.00/0